

Effect of Gamma Radiation on Electrical Properties of $\text{Bi}_{1-x}\text{Ca}_x\text{FeO}_3$ Multiferroic

A. M. Madbouly

Egyptian Nuclear and Radiological Regulatory Authority, Postal code: Nasr City 11762, P.O.Box. 7551., Cairo, Egypt

Abstract: $\text{Bi}_{1-x}\text{Ca}_x\text{FeO}_3$; ($0.0 \leq x \leq 0.4$) (BCFO) multiferroic samples were prepared in single phase using flash auto combustion method. Investigation of dielectric constant and ac conductivity of the samples was carried out. Frequency dependent dielectric constant, dielectric loss and ac conductivity measurement from $10^2 - 10^6$ Hz at room temperature shows usual dielectric dispersion behavior before and after γ -irradiation. The results promote the use of the γ -irradiated multiferroics in high frequency applications.

Keywords: multiferroics, gamma radiation, dielectric

1. Introduction

Multiferroic materials exhibiting coexistence and simultaneous coupling of ferroelectricity and ferromagnetism have recently attracted considerable attention due to their potential applications and attractive physical phenomena [1–3]. As one of representative single-phase multiferroics, BiFeO_3 (BFO) is known to be the only material that is both ferroelectric ($T_C \sim 1103$ K) and antiferromagnetic ($T_N \sim 643$ K) at room temperature, which makes it an excellent possible candidate for practical application [4].

BiFeO_3 (BFO) is one of the most important multiferroics in the views of the applications perspective and engineering possibilities [5, 6]. Highly ferroelectric ordering temperature and magnetic ordering temperature make it as an attractive candidate for bifunctional device applications in the emerging field of spintronics [7].

The perovskite-like BiFeO_3 compound, in which the stereochemical activity of the Bi lone electron pair gives rise to ferroelectric polarization, while the partially filled 3d orbitals of the Fe^{3+} ions cause G-type antiferromagnetic order, seems to be one of the most suitable objects for multiferroic research in view of its high magnetic and ferroelectric ordering in a wide temperature range ($T_N \sim 640$ K, $T_C \sim 1100$ K) has attracted much attention, and encouraged scientists to design, develop and characterize BiFeO_3 -based and other materials for multi-functional applications on magnetoelectric sensors, optic and microwave devices [8,9].

2. Experimental Technique

$\text{Bi}_{1-x}\text{Ca}_x\text{FeO}_3$ ($0.0 \leq x \leq 0.4$) (BCFO) was prepared by the flash auto combustion technique using high-purity bismuth nitrate $\text{Bi}(\text{NO}_3)_3 \cdot 5\text{H}_2\text{O}$, calcium nitrate $\text{Ca}(\text{NO}_3)_2 \cdot 4\text{H}_2\text{O}$, iron nitrate $\text{Fe}(\text{NO}_3)_3 \cdot 9\text{H}_2\text{O}$ and urea. The amount of urea was calculated using charge neutrality [10]. The chemicals were weighed in the required stoichiometric proportions and mixed together for a few minutes. The reactants were hand mixed and heated on a magnetic stirrer. Thermal dehydration resulted in a highly viscous liquid. On further heating at high temperature, the viscous liquid swelled and auto-ignited, to produce voluminous powder. The reaction

was too fast and produced dry very fine powder. This method is quite simple, fast and inexpensive and exploits an exothermic, usually very rapid and self sustaining chemical reaction between the desired metal salts and a suitable organic fuel, usually urea. The obtained nanopowders were heated at 500°C for 4 hrs using a heating/cooling rate of $4^\circ\text{C}/\text{min}$.

$\text{Bi}_{1-x}\text{Ca}_x\text{FeO}_3$ samples were irradiated by Co^{60} – radiation of dose 1.7Mev at the Technological Research Center of radiation (Nasr city, Cairo). All measurements were performed before as well as after irradiation. The RLC Bridge (Hioki model 3530 Japan) was used to measure the ac electrical resistivity of the investigated samples. The dielectric constant (ϵ'), dielectric loss factor (ϵ'') and, $\tan\delta$ for the samples were measured from room temperature up to 800 K at different frequencies ranging from 600 kHz to 5000 kHz. The temperature of the sample was measured using copper constantan thermocouple connected to Digi-sense thermometer (USA) with junction in contact with the sample. The accuracy of measuring temperature was also better than $\pm 1^\circ\text{C}$.

3. Results and Discussion

Fig. 1 shows the XRD patterns of $\text{Bi}_{1-x}\text{Ca}_x\text{FeO}_3$ with different content ($0.0 \leq x \leq 0.4$). The diffraction peaks and relative intensities (I/I_0) in all samples were indexed and reported in Table 1 in comparison with ICDD card number 82-1254. The crystal structure is rhombohedral, and could be described structure in a hexagonal frame of reference with R3c space group. No impurity phase was found in these samples, which means that all samples were analyzed single phase. A slight shift in the peaks to a greater 2θ angle is observed when Ca^{2+} ions are introduced in BFO indicating the decrease in the unit cell volume. The doubly split peaks of BFO in the 2θ ranges of 31-33 and 38-41 merge partially to form a broadened one in BCFO.

The lattice parameter (a) decreased as the Ca doping increases. This can be understood in terms of smaller ionic size of Ca^{2+} (1.12 \AA) in comparison with that for Bi^{3+} (1.17 \AA) ion [11]. The lattice parameter c is nearly constant in agreement ICDD card.

Fig.2 (a-c) shows the frequency dependence of ac conductivity (σ), dielectric constant (ϵ') and dielectric loss tangent ($\tan\delta$) of $\text{Bi}_{1-x}\text{Ca}_x\text{FeO}_3$ (where $0.0 \leq x \leq 0.4$) in range 100Hz to 1MHz at room temperature. The decrease in the (ϵ') is rapid at lower frequencies and slower at higher frequencies. The decrease in (ϵ') with increasing in frequency is a normal dielectric behavior. This normal dielectric behavior is also observed by several other investigations [12, 13]. The dielectric constant decreases with increasing frequency, and could be explained by the phenomenon of dipole relaxation where at low frequencies the dipoles are able to follow the frequency of the applied field [14-16]. Also the behavior can be qualitatively explained in the following way [17, 18], the oxygen vacancies- related dipoles follow the alternating field at low frequencies, providing high values of (ϵ'), but lag is obtained behind the field in the high frequency range. It is clear from the figure that Ca-doping reduces drastically the frequency dispersion of BiFeO_3 and it is minimum for $\text{Bi}_{0.9}\text{Ca}_{0.1}\text{FeO}_3$ sample. The high dielectric constant of calcium doped BiFeO_3 as compared to the pure BiFeO_3 can be attributed to higher space charge polarization for first one. Fig. 1b shows the dependence of dissipation factor ($\tan\delta$) for the above composition with frequency. At higher frequencies the dissipation factor ($\tan\delta$) is of order of 10^{-1} . The low loss at

higher frequencies identifies the potential of these multiferroics for high frequency applications [19]. Fig.1c shows the variations of the ac conductivity as a function of frequencies. The ac conductivity increased with increasing in frequency. Owing to charge compensation, doping bivalent cations (such as Ca^{2+} , Pb^{2+} and Ba^{2+}) would give rise to the formation of Fe^{4+} or oxygen vacancies [20, 21]. When Ca substitutes Ba^{3+} in BiFeO_3 , the exchange between Fe^{4+} and Fe^{3+} takes place in a local displacement in the direction of the applied field and increasing the dielectric constant and conductivity.

Figs. (3a-c) and (4a-c) shows the temperature dependence of the real part of the dielectric constant (ϵ') and dielectric loss tangent ($\tan\delta$) for the unirradiated and γ -irradiated $\text{Bi}_{1-x}\text{Ca}_x\text{FeO}_3$ ($x = 0.0, 0.1$ and 0.3) with dose of 2MeV. From this figure the observed peak around 668K corresponds to the transition from antiferromagnetic to paramagnetic phase at the Neel temperature [22]. This phase transition is observed on as an abnormal peak in the dielectric constant (T_N) and dielectric loss tangent ($\tan\delta$) versus temperature as shown Figs. (5a-c) and (6a-c). Another peak around 400K is also observed, which seems to agree with the dielectric measurements [23].

Table 1: The calculated d-spacing of the recorded peaks and the corresponding relative intensities I/I_0 in comparison with the data of the ICDD card.

Bi-ferrite (ICDD card) 82-1254			X=0		X=0.1		X=0.2		X=0.3		X=0.4	
Plane	d(A)	$I/I_0\%$	d(A)	$I/I_0\%$	d(A)	$I/I_0\%$	d(A)	$I/I_0\%$	d(A)	$I/I_0\%$	d(A)	$I/I_0\%$
012	3.9628	87	3.96007	53.6	3.9423	27.4	3.92123	23.4	3.91815	19.47	3.9155	20.9
104	2.8157	98	2.81236	96.4	-	-	-	-	-	-	-	-
110	2.7887	100	2.78752	100	2.78820	100	2.77338	100	2.76852	100	2.76888	100
113	2.3875	1.3	-	-	-	-	-	-	-	-	-	-
006	2.3102	8.7	2.30674	11.8	2.27412	25.3	2.26381	20.6	2.26032	11.81	2.26047	15.8
202	2.2806	29.5	-	-	-	-	-	-	-	-	-	-
024	1.9814	4.8	1.97857	33	1.97330	16.4	1.96117	22.6	1.95722	23	1.95840	18.8
211	1.8100	0.4	-	-	-	-	-	-	-	-	-	-
116	1.7790	28.8	1.77830	27.4	1.76885	11	1.75302	6.8	1.74988	-	-	-
122	1.7654	15.5	-	-	-	-	-	-	-	-	-	-
018	1.6309	14.4	-	-	-	-	-	-	-	-	-	-
214	1.6152	33.9	1.61233	36	1.60578	26.5	1.60112	27.7	1.59928	22.12	1.59904	27.5
300	1.6100	28.9	-	-	-	-	-	-	-	-	-	-
125	1.5247	0.1	-	-	-	-	-	-	-	-	-	-
208	1.4078	6.3	-	-	-	-	-	-	-	-	-	-
220	1.3943	11.4	1.39118	8.5	1.39380	9.5	1.38645	9.5	1.3843	12.38	1.38445	10
036	1.3209	8.4	1.32704	9.8	1.31439	8.9	1.30539	3.5	1.32704	9.8	1.31439	8.9
312	1.3153	5.6	-	-	-	-	-	-	-	-	-	-
128	1.2567	9.3	1.25246	10.1	1.24747	9.2	1.24155	4.7	1.2378	7	1.23789	6.3
134	1.2495	10.9	-	-	-	-	-	-	-	-	-	-

The variation of the electrical conductivity for the investigated compositions vs $10^3/T$ at frequencies (100, 10^3 , 10^4 and 10^5 Hz) is shown in Figs. (7a-c) and (8a-c) for the unirradiated and irradiated $\text{Bi}_{1-x}\text{Ca}_x\text{FeO}_3$. The conductivity was observed to increase as the temperature increased from 298 K attaining a maximum around 398 K for $x = 0.1$, after which the conductivity was found to decrease and reached a minimum around 460 K beyond which the conductivity showed an increase again. These temperatures are depending on Ca^{2+} ions concentration. The nature of variation of conductivity with temperature is found to be similar as reported in [24]. The first increase in conductivity at

relatively low temperature is due to impurities but at high temperature is due to hopping of charge carriers according to the band theory. The charge transfer gap is directly correlated to the orbital overlap between the oxygen p orbitals and the iron d orbitals, the overlap being highly pronounced also bigger when the Fe – O – Fe angle is straighter [25]. Accordingly, it is expected that the bandgap of Ca – doped BFO should be considerably lower than that of pure BFO, leading to much increased conductivity. Also the increase in the dielectric permittivity and loss factor with increasing temperature is then related to the thermally induced enhancement of the conductivity. It is expected that γ

irradiation leads to the formation of oxygen vacancies. Consequently some of Fe^{3+} keep their trivalent state and thus decrease the chance of Fe^{4+} formation which lowers the conductivity.

4. Conclusion

BCFO were prepared in single phase using flash auto combustion method and were as fuel. Ca^{2+} doping leads to a decrease in the unit cell parameter. The values of dielectric constant, dielectric loss factor, and ac conductivity decreased after γ -irradiation. One could recommend the use of these multiferroics in high frequency applications due to their negligible loss.

5. Acknowledgments

The author would like to extend her gratitude to Dr. Salwa Faheem from faculty of science in Zagazig University and Proff. Dr. Mohamed Aly from faculty of science in Cairo University for their valuable helps.

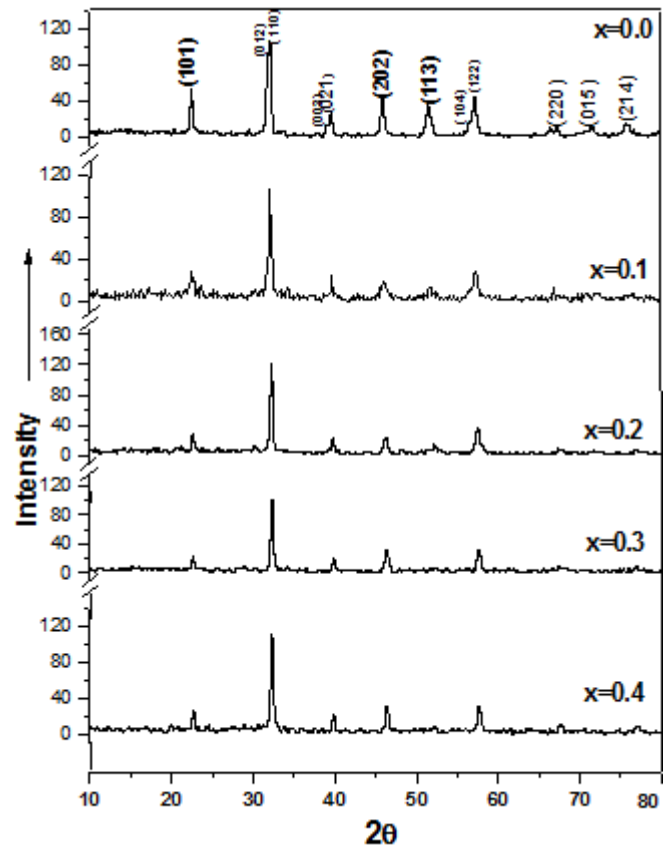


Figure 1: The X-ray diffraction pattern obtained for $\text{Bi}_{1-x}\text{Ca}_x\text{FeO}_3$ ($0.0 \leq x \leq 0.4$)

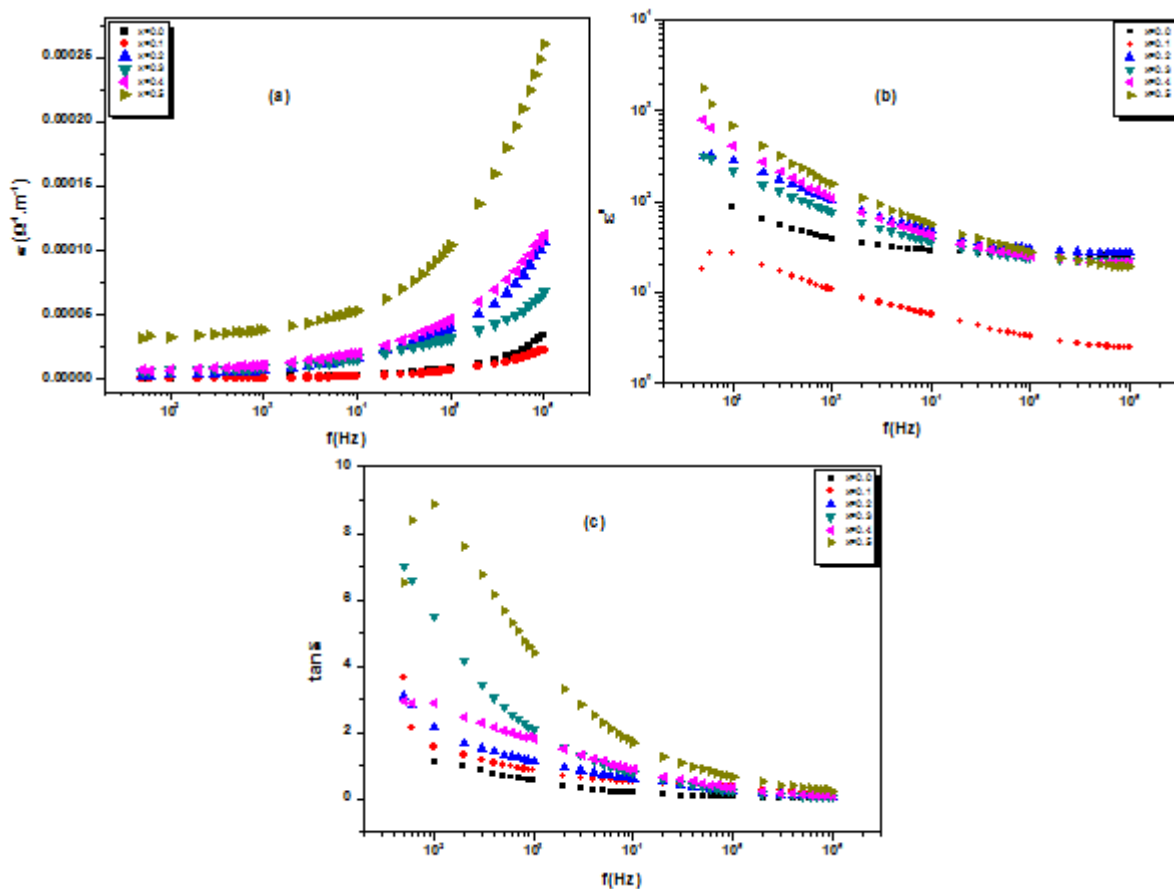


Figure 2(a-c): Dependences of ac conductivity, dielectric constant and dielectric loss on frequency $\text{Bi}_{1-x}\text{Ca}_x\text{FeO}_3$ ($x = 0.0, 0.2, 0.3$ and 0.4)

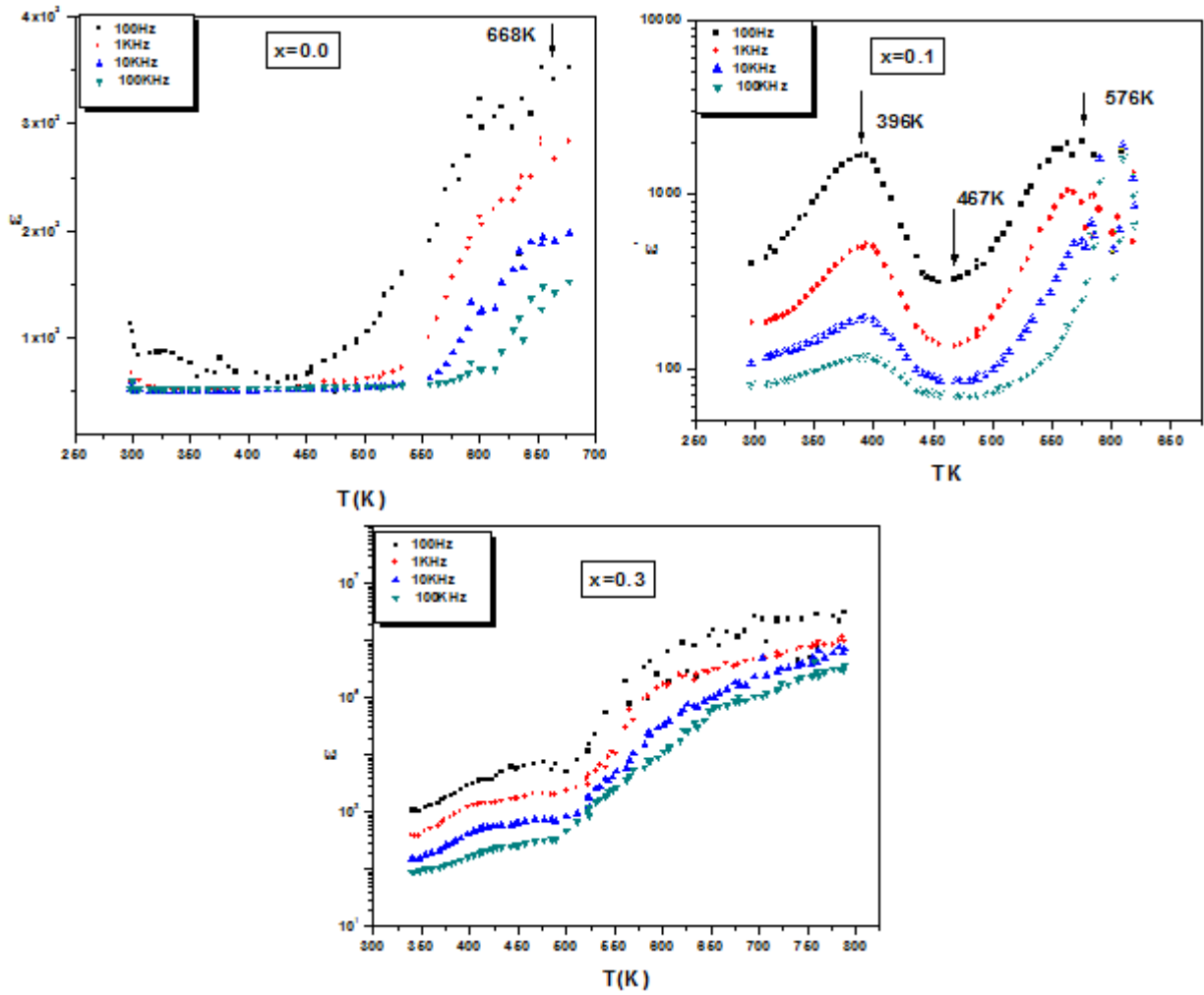
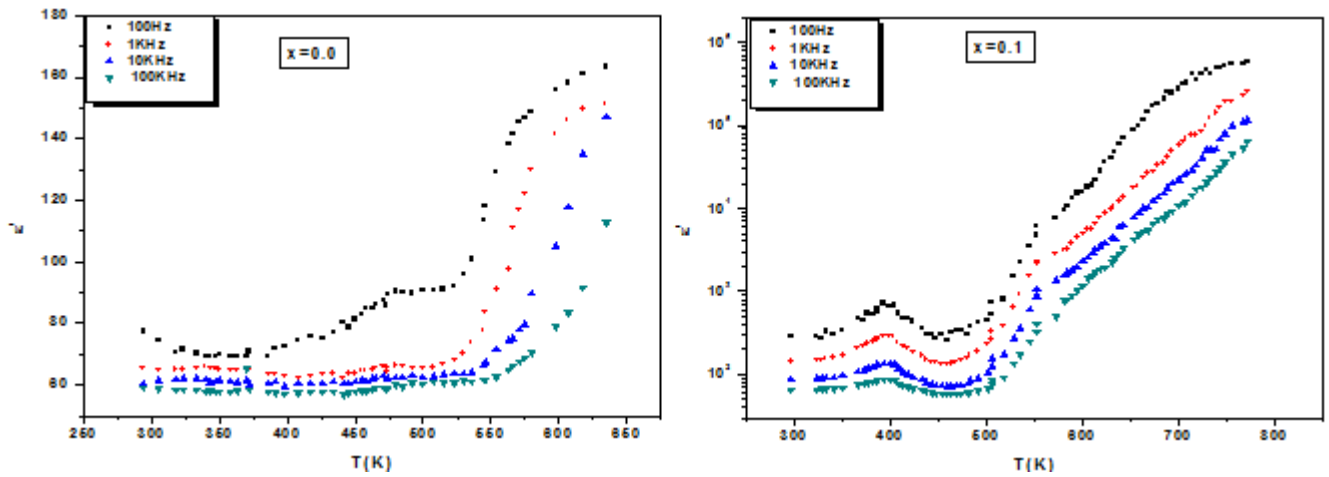


Figure 3(a-c): Dependence of dielectric constant on absolute temperature before irradiation.



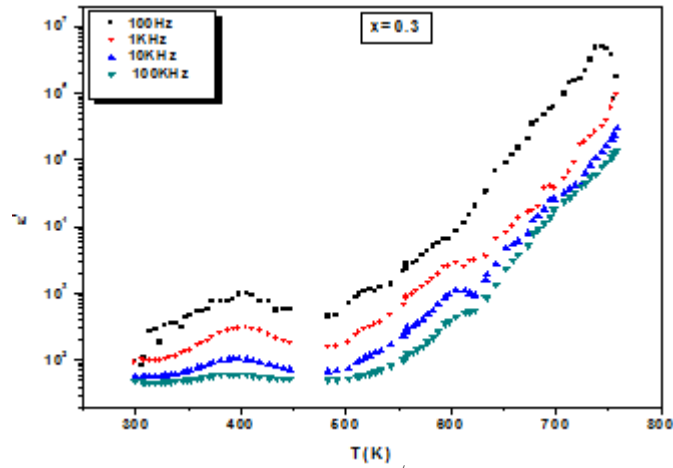


Figure 4(-c) a: Dependence of dielectric constant (ϵ') on absolute temperature after irradiation.

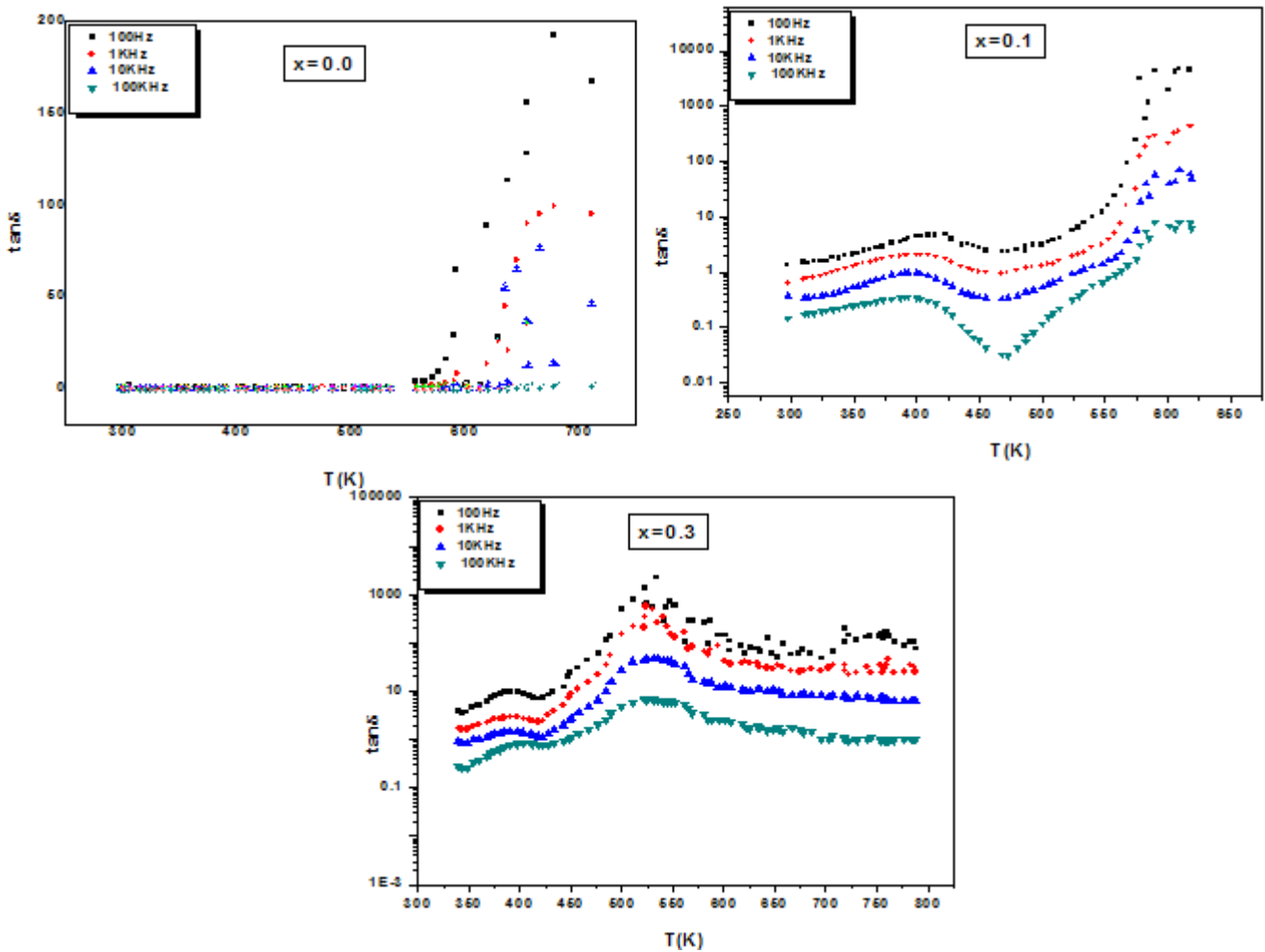


Figure 5(a-c): Dependence of dielectric loss ($\tan\delta$) on absolute temperature before irradiation

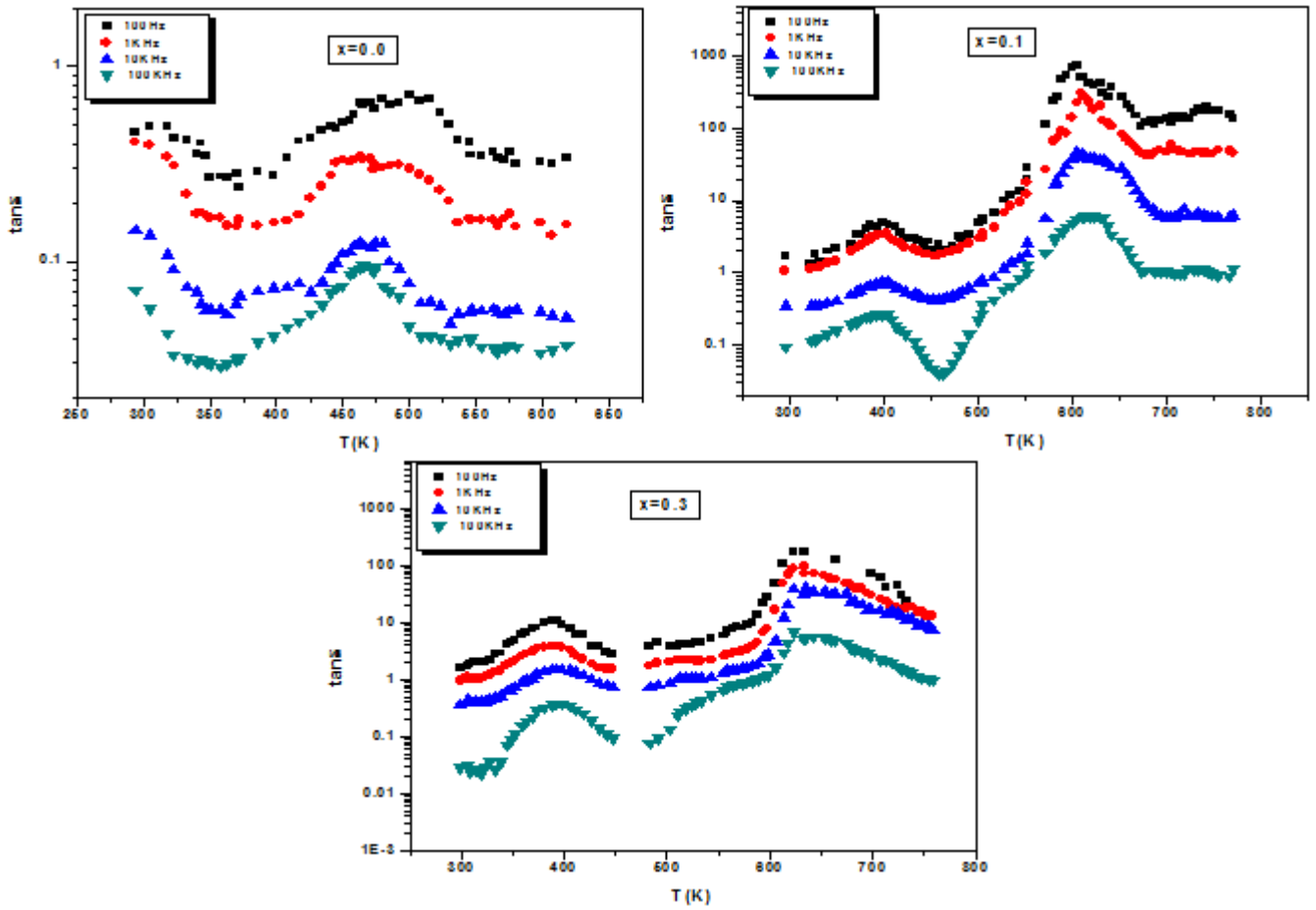


Figure 6(a-c): Dependence of dielectric loss ($\tan\delta$) on absolute temperature after irradiation.

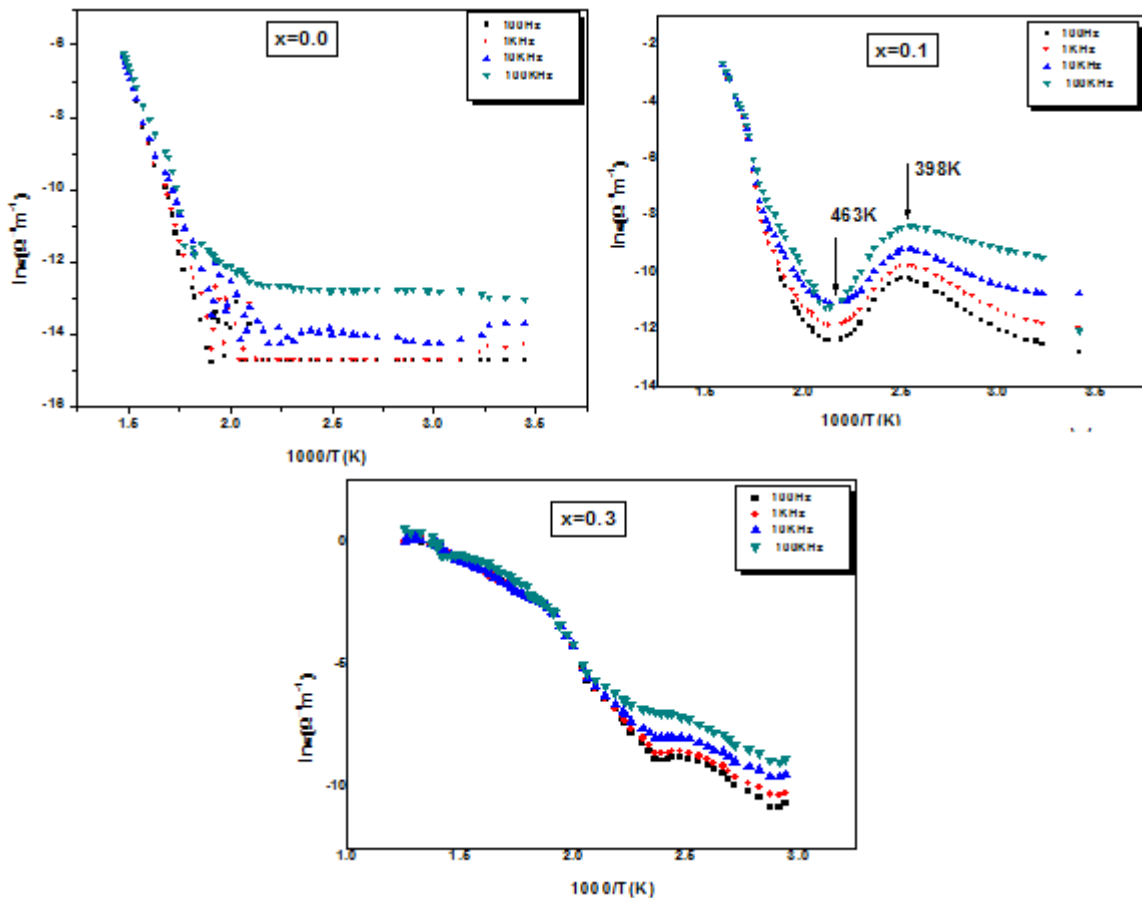


Figure 7(a-c): Dependence of ac conductivity (σ) on absolute temperature before irradiation.

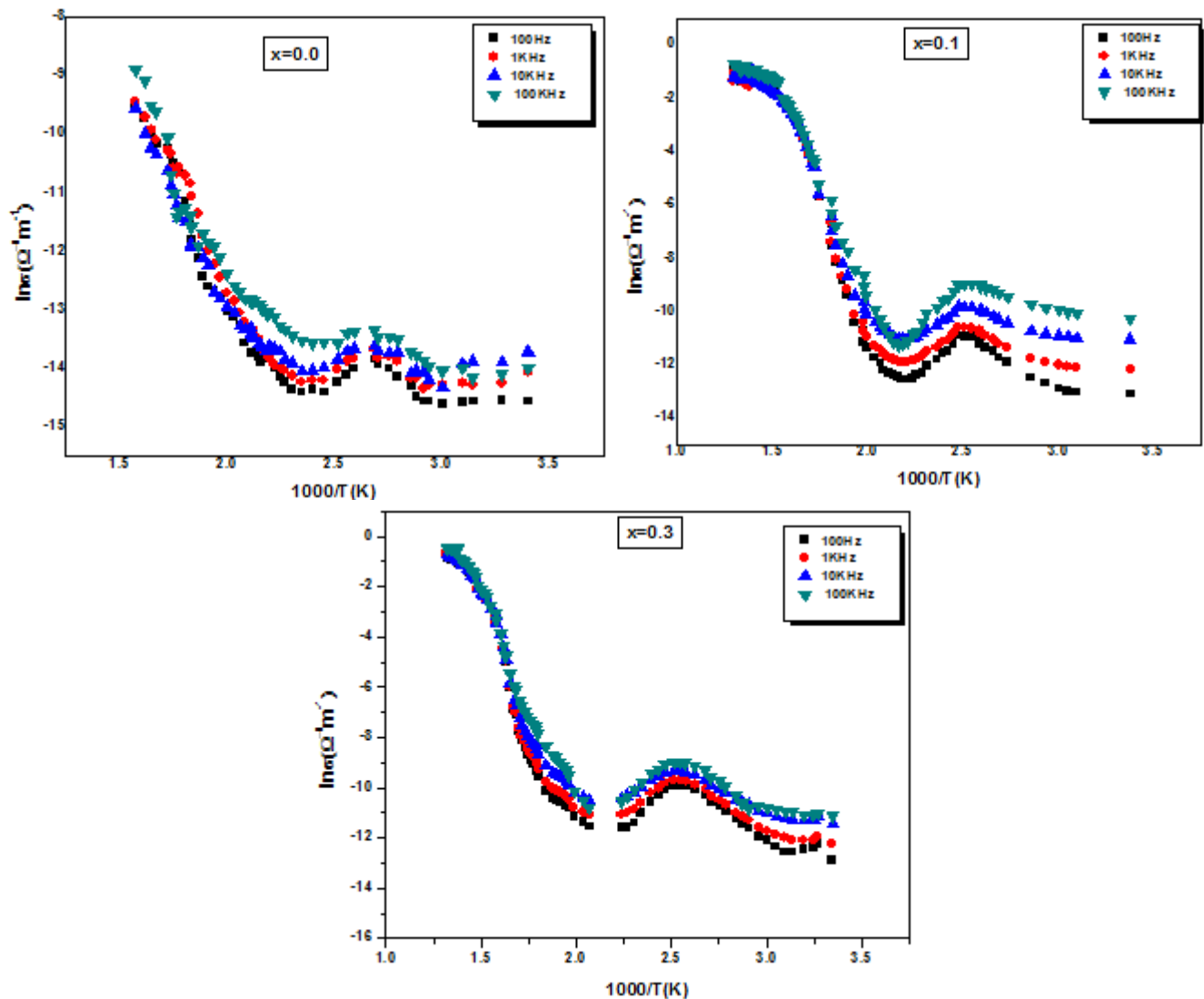


Figure 8(a-c): Dependence of ac conductivity (σ) on absolute temperature after irradiation.

References

- [1] M. Fiebig, J. Phys. D 38 (2005) R123.
- [2] K.F. Wang, J.M. Liu, Z.F. Ren, Adv. Phys. 58 (2009) 321.
- [3] C.W. Nan, M.I. Bichurin, S.X. Dong, D. Viehland, G. Srinivasan, J. Appl. Phys. 103 (2008) 031101.
- [4] J. Wang, J.B. Neaton, H. Zheng, V. Nagarajan, S.B. Ogale, B. Liu, D. Viehland,
- [5] V. Vaithyanathan, D.G. Schlom, U.V. Waghmare, N.A. Spaldin, K.M. Rabe, M. Wuttig, R. Ramesh, Science 299 (2003) 1719.
- [6] H. Béa, M. Bibes, M. Bibes, F. Ott, B. Dupé, X.H. Zhu, S. Petit, S. Fusil, C. Deranlot, K. Bouzehouane, A. Barthélémy, Phys. Rev. Lett. 100 (2008) 017204.
- [7] H.W. Jang, S.H. Baek, D. Ortiz, C.M. Folkman, R.R. Das, Y.H. Chu, P. Shafer, J.X. Zhang, S. Choudhury, V. Vaithyanathan, Y.B. Chen, D.A. Felker, M.D. Biegalski, M.S. Rzhowski, X.Q. Pan, D.G. Schlom, L.Q. Chen, R. Ramesh, C.B. Eom, Phys. Rev. Lett. 101 (2008) 107602.
- [8] N.A. Spaldin, M. Fiebig, Science 309 (2005) 391.
- [9] N.A. Hill, J. Phys. Chem. B 104 (2000) 6694.
- [10] M. Fiebig, Th. Lottermoser, D. Frohlich, A.V. Golsev, R.V. Pisarev, Nature (London) 419 (2002) 819.
- [11] M.A. Ahmed, N. Okasha and S.I. El-Dek, Nanotechnol. 19 (2008) p.065603.
- [12] R.D. Shanon, Acta Crystallogr. A 32 (1976) 751.
- [13] Jyoti Ranjan Sahu, C.N.R. Rao, Solid State Sciences 9(2007) 950.
- [14] H. O. Rodrigues, G.F.M. Pires Junior, J. S. Almeida, E. O. A.C. Rodrigues, M.A.S. Silva, A.S.B. Sombra, J. of Physics and Chemistry of Solids, 71 (2010) 1329.
- [15] D.H. Wang, W.C. Goh, M. Ning, C. K. Ong, Appl. Phys. Lett. 88 (2006) 212907.
- [16] M. Kumar, K. L. Yadav, J. Phys. 100 (2006) 74111.
- [17] M. Kumar, K. L. Yadav, J. Phys. Condens. Matter 18 (2006) L503.
- [18] G. I. Yuan, S.W. Or, J. Appl. Phys. 100 (2006) 024109.
- [19] A. Dutra, T.P. Sinha, J. Phys. Chem. Solids 67 (2006) 1484.
- [20] T.T. Ahmed, I.Z. Rahman, M.A. Rahman, J. Mater. Process, Technol. 152-154(2004) 797.
- [21] D.H. Wang, W.C. Goh, M. Ning, C.K. Ong, Appl. Phys. Lett. 84 (2004) 1731.
- [22] V.A. Khomchenko, D.A. Kiselev, M. Kopcewicz, M. Maglione, V.V. Shvartsman, P. Borisov, W. Kleemann,

- A.M.L. Lopes, Y.G. Pogorelov, J.P. Araujo, R.M. Rubinger, N.A. Sobolev, J.M. Vieira, A.L. Kholkin, J. Magn. Mater. 321 (2009) 1692.
- [23] J. M. Moreau, C. Michel, R. Gerson, and W.J. James, *J. Phys. Chem. Solids*, **32**(1971) 1315.
- [24] W.M. Zhu, and Z.G. Ye, *Ceram. Int.*, 30 (2004)1435.
- [25] A. Hussain, A. Begum, and A. Rahman, *Journal of Optoelectronics and Advanced Materials*, 12 (2010) 1019.
- [26] S.A.T. Redfern, J.N. Walsh, S.M. Clark, G. Catalan, J. F. Scott, arXiv:0901.3748v2. (2009).